

Dioxomorpholines and Derivatives from a Marine-Facultative *Aspergillus* Species

By: Manuel A. Aparicio-Cuevas, Isabel Rivero-Cruz, Mariano Sánchez-Castellanos, Daniel Menéndez, [Huzefa A. Raja](#), Pedro Joseph-Nathan, María del Carmen González, and [Mario Figueroa](#)

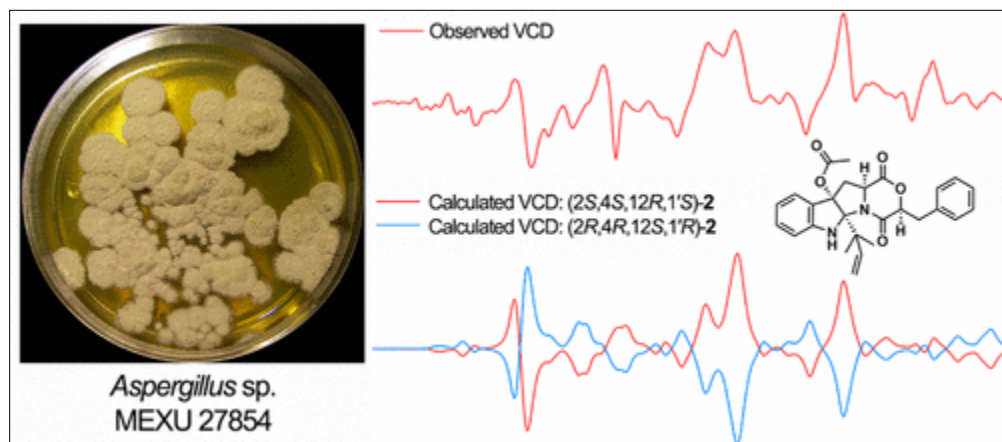
Aparicio-Cuevas, M.A., Rivero-Cruz, I., Sánchez-Castellanos, M., Menéndez, D., Raja, H.A., Joseph-Nathan, P., del Carmen González, M., Figueroa, M. (2017). Dioxomorpholines and Derivatives from a Marine-Facultative *Aspergillus* Species. *Journal of natural products*, 80(8), 2311-2318.

Made available courtesy of American Chemical Society:

<http://dx.doi.org/10.1021/acs.jnatprod.7b00331>

***© American Chemical Society and American Society of Pharmacognosy. Reprinted with permission. No further reproduction is authorized without written permission from American Chemical Society. This version of the document is not the version of record. Figures and/or pictures may be missing from this format of the document. ***

Abstract:



Two new dioxomorpholines, 1 and 2, three new derivatives, 3–5, and the known compound PF1233 B (6) were isolated from a marine-facultative *Aspergillus* sp. MEXU 27854. Their structures were established by 1D and 2D NMR and HRESIMS data analysis. The absolute configuration of 1 and 2 was elucidated by comparison of experimental and DFT-calculated vibrational circular dichroism spectra. Compounds 3, 5, and 6 were noncytotoxic to a panel of human cancer cell lines with different functional status for the tumor-suppressor protein p53, but were inhibitors of P-glycoprotein-reversing multidrug resistance in a doxorubicin-resistant cell line.

Keywords: Biochemistry | *Aspergillus* | Dioxomorpholines

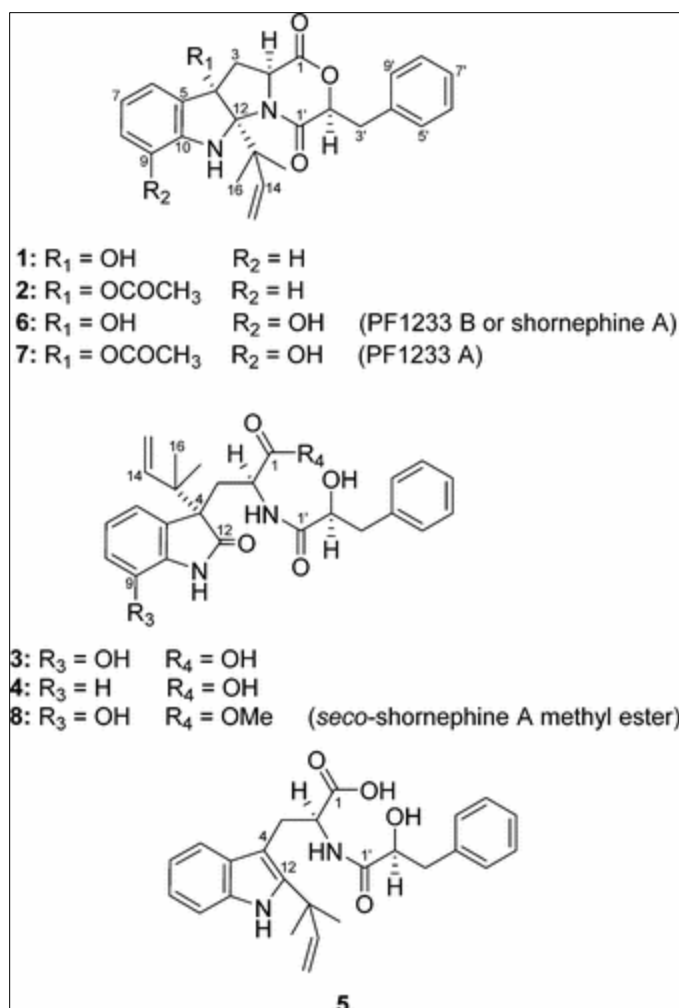
Article:

The genus *Aspergillus* consists of over 300 species distributed worldwide. Some of these species are pathogenic in humans and animals; others are saprophytic molds that can be found in oligotrophic or extreme environments.(1) Marine-derived *Aspergillus* species have proven to be an excellent source of biologically active molecules with pharmaceutical relevance and structurally diverse scaffolds.(2-5)

During our search for new secondary metabolites from unexplored sources, we found that a marine-facultative *Aspergillus* sp. MEXU 27854 from Caleta Bay in Acapulco, Guerrero, Mexico, produces two new dioxomorpholines, **1** and **2**, along with three new derivatives, **3–5**, and the known compound PF1233 B (**6**).(6) An extensive literature search revealed that the morpholine-2,5-dione ring system is rare in Nature and most commonly found in compounds from fungi.(7-15)Recently, PF1233 B (**6**) was isolated from *Aspergillus niveus* in 2003 as a novel inhibitor of voltage-dependent sodium channels,(6) but it was reported again as a new natural product (shornephine A) and P-glycoprotein (Pgp) inhibitor in 2014 by Khalil and collaborators.(15)

Drug resistance to chemotherapeutic agents is one of the major hurdles in cancer therapy. The multidrug resistance phenotype (MDR) of tumor cells exhibits reduced sensitivity to a large group of unrelated drugs with different mechanisms of pharmacological activity. MDR is also responsible for resistance to an extensive variety of chemotherapeutic/anticancer drugs.(16) Two of the major contributors to drug resistance are the overexpression of membrane-bound drug transporter proteins, such as Pgp and multidrug resistance-associated proteins (MRP1 and MRP2),(17) and suppression of apoptosis or cell cycle arrest, due to inactivation of wild-type function and/or mutation of the tumor suppressor p53, also known as the guardian of the genome.(18, 19) Several studies have established a functional crosstalk between these two pathways of drug resistance.(20-23)

In this work, we describe the characterization of compounds **1–5** by 1D and 2D NMR data analysis. Additionally, the absolute configuration of dioxomorpholines **1** and **2** was determined by comparison of the experimental and DFT-calculated vibrational circular dichroism (VCD) spectra. We also characterized the cytotoxic properties of **3**, **5**, and **6** and further explored their effects using a panel of cancer cell lines with different p53 functional status and against a multidrug resistance cell line that overexpresses Pgp and presents doxorubicin resistance.



Results and Discussion

The defatted organic extract of a rice-based culture of the marine-facultative *Aspergillus* sp. MEXU 27854 was extensively chromatographed to yield PF1233 B (**6**), (**6**, 15) the new dioxomorpholines **1** and **2**, and three new derivatives, **3–5**. The fungal strain was isolated from a sample of sand collected in a transition zone between land and sea at Caleta Bay, Acapulco, Guerrero, Mexico, and was identified using both morphology and molecular analysis of the ITS1-5.8S-ITS2 and partial calmodulin regions (Supporting Information and Figure S1).

Compound **1** was obtained as a yellow oil. Its molecular formula was deduced as C₂₅H₂₆N₂O₄ based on its molecular ion peak in the HRESIMS, establishing an index of hydrogen deficiency (IHD) of 14. Detailed analysis of the 1D and 2D NMR data (Table 1 and Figure 1) suggested that **1** lacks of the phenolic hydroxy group at C-9 (δ_c 111.1) when compared to the known dioxomorpholine PF1233 B (**6**) (δ_c 141.6, C-9). The ¹H NMR spectrum (Figure S7) exhibited nine aromatic protons, three methine, three methylene, and two methyl groups, and one NH proton. The ¹³C and HSQC spectra (Figures S7 and S9) revealed the presence of 25 carbons that were assigned as two carbonyl, 12 aromatic (nine protonated), two methyl, three methylene, three methine, a tertiary oxygenated sp³ carbon, one quaternary, and a carbon atom flanked by

two heterocyclic nitrogens. COSY data confirmed the five spin systems of **1** (nine aromatic protons indicating the presence of an indoline unit and a monosubstituted benzene ring, and three systems composed of a methylene adjacent to a methine group), and the remaining connectivities were determined by detailed analysis of HMBC correlations (Figure 1). On the basis of these considerations, compound **1** was given the trivial name 9-deoxy-PF1233 B.

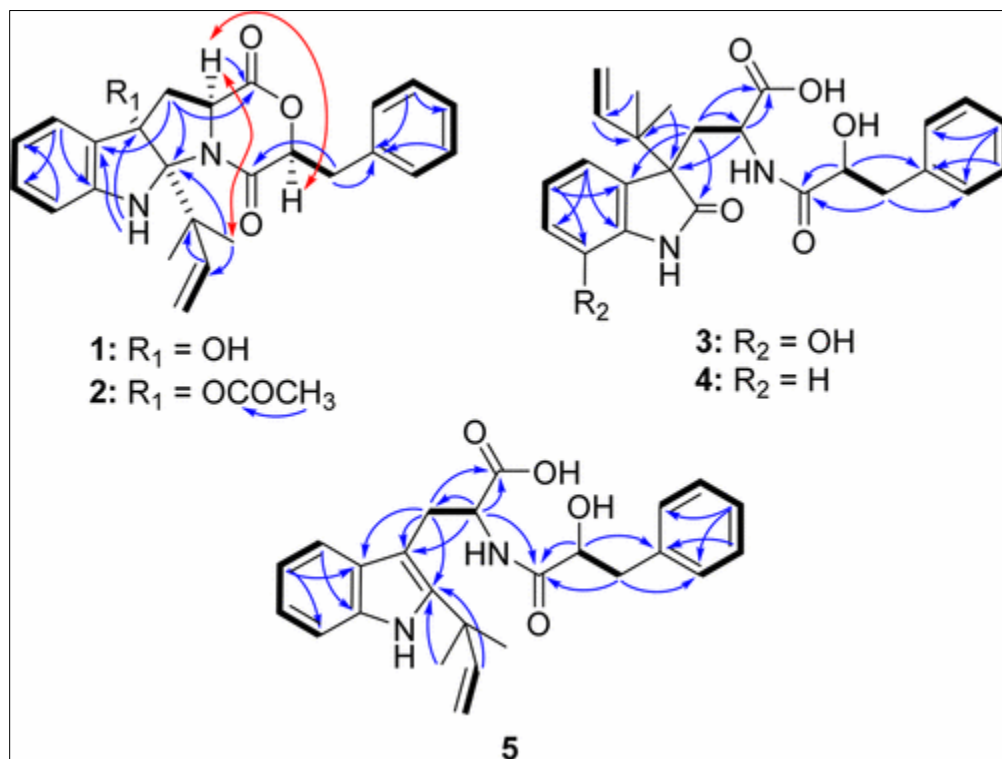


Figure 1. Selected key COSY (bold lines), HMBC (→), and NOESY (↔) correlations of **1–5**.

Table 1. ¹H and ¹³C NMR Data for Compounds **1** and **2** in CDCl₃

position	1^a			2^b		
	δ _C , type	δ _H , mult. (<i>J</i> in Hz)		δ _C , type	δ _H , mult. (<i>J</i> in Hz)	
1	167.4, C			167.0, C		
2	57.2, CH	4.34, dd (10.3, 1.7)		58.4, CH	4.35, dd (10.4, 1.7)	
3	36.9, CH ₂	3.28, dd (13.7, 1.7)		34.8, CH ₂	4.19, dd (14.0, 1.7)	
		2.83, dd (13.7, 10.3)			2.78, dd (14.0, 10.4)	
4	88.0, C			91.1, C		
4-OH		^c				
5	128.9, C			125.6, C		
6	124.8, CH	7.29, d (7.5)		128.6, CH	7.61, d (7.4)	
7	120.7, CH	6.82, td (7.5, 1.2)		120.3, CH	6.77, t (7.4)	
8	131.0, CH	7.16, td (7.5, 1.2)		131.1, CH	7.14, t (7.8)	
9	111.1, CH	6.68, d (7.5)		110.8, CH	6.66, d (7.8)	
10	147.8, C			148.7, C		

11-NH			6.29, bs			6.28, bs
12	94.7,	C		98.3,	C	
13	45.0,	C		45.2,	C	
14	143.9,	CH	6.36, dd (17.8, 10.9)	144.0,	CH	6.30, dd (17.6, 10.7)
15	113.9,	CH ₂	5.19, dd (17.8, 1.2)	112.8,	CH ₂	5.14, dd (17.6, 1.2)
			5.12, dd (10.9, 1.2)			5.10, dd (10.7, 1.2)
16	23.3,	CH ₃	1.37, s	24.9,	CH ₃	1.42, s
17	26.1,	CH ₃	1.35, s	25.5,	CH ₃	1.35, s
18				168.7,	C	
19				21.6,	CH ₃	1.98, s
1'	166.1,	C		166.0,	C	
2'	78.6,	CH	4.77, dd (8.5, 3.4)	78.3,	CH	4.73, dd (9.0, 3.4)
3'	34.8,	CH ₂	3.33, dd (14.9, 3.4)	34.6,	CH ₂	3.31, dd (15.4, 3.4)
			2.88, dd (14.9, 8.5)			2.84, dd (15.4, 9.0)
4'	136.2,	C		136.0,	C	
5'/9'	128.6,	CH	7.22, m	128.4,	CH	7.19, d (7.4)
6'/8'	129.6,	CH	7.22, m	129.4,	CH	7.19, d (7.4)
7'	127.0,	CH	7.21, m	126.9,	CH	7.23, m

^a 500 MHz for ¹H and 125 MHz for ¹³C. ^b 700 MHz for ¹H and 175 MHz for ¹³C. ^c Not observed.

Compound **2** was isolated as a yellow oil and, based on the HRESIMS analysis, had the molecular formula C₂₇H₂₈N₂O₅ (IHD = 15). The NMR data (Table 1 and Figure 1) suggested a structural similarity to **1** and the known dioxomorpholine PF1233 A (**7**);(6) the key differences were the presence of an acetyl group [δ_{H} 1.98 (3H, s, H₃-19) and δ_{C} 168.7 (C-18) and 21.6 (C-19)], as well as the ¹³C NMR shift of C-4 that was deshielded to δ_{C} 91.1. The presence of this group was also supported by the 42 Da difference in the HRMS comparative analysis between **1** and **2**. The acetylated derivative of **1** was thus given the trivial name 9-deoxy-PF1233 A (**2**).

Compound **3** was obtained as a pale yellow oil, and its molecular formula deduced as C₂₅H₂₈N₂O₆ by HRESIMS analysis (IHD = 13). 1D and 2D NMR data (Table 2) for this compound were nearly identical to those of known *seco*-shornephine A methyl ester (**8**).(6, 15) COSY data (Figure 1) confirmed three freely rotating spin systems having a methylene adjacent to a methine group, and the HMBC spectrum (Figure S20) showed strong correlations from H₂-3 to C-12, C-13, C-4, C-2, and C-5; from H₃-16 and H₃-17 to C-4, C-13, and C-14; and from H-14 to C-13, C-16, and C-17. The difference of 14 Da from **8**, the lack of NMR signals for a methyl ester [δ_{H} 3.35 (3H, s, 1-OMe) and δ_{C} 52.1 in **8**], and the downfield shifted C-1 (δ_{C} 176.3 and 172.5 for **3** and **8**, respectively) supported the presence of a carboxylic acid functionality in compound **3**. This compound was therefore named *seco*-PF1233 B carboxylic acid (**3**).

Table 2. ¹H and ¹³C NMR Data for Compounds 3–5 in CD₃OD

position	3 ^a			4 ^b			5 ^a		
	δ _C , type		δ _H , mult. (<i>J</i> in Hz)	δ _C , type		δ _H , mult. (<i>J</i> in Hz)	δ _C , type		δ _H , mult. (<i>J</i> in Hz)
1	176.3, C			175.5, C			177.5, C		
1-OH									
2	51.8, CH		3.99, dd (10.6, 2.3)	51.3, CH		3.92, dd (10.3, 2.3)	55.7, CH		4.75, dd (10.4, 5.3)
3	34.0, CH ₂		2.59, dd (14.2, 2.3)	33.3, CH ₂		2.63, dd (14.2, 2.3)	29.0, CH ₂		3.39, dd (14.6, 5.3)
			2.39, dd (14.2, 10.6)			2.38, dd (14.2, 10.3)			3.12, dd (14.6, 10.4)
4	58.6, C			56.8, C			106.8, C		
5	131.1, C			128.9, C			131.1, C		
6	116.2, CH		6.72, d (7.8)	126.4, CH		7.32, d (7.4)	119.7, CH		7.60, dd (7.6, 1.4)
7	123.2, CH		6.80, t (7.8)	121.2, CH		7.02, t (7.4)	119.4, CH		7.03, m
8	118.8, CH		6.78, d (7.8)	127.9, CH		7.19, t (7.4)	121.7, CH		7.03, m
9	142.9, C			109.3, CH		6.83, d (7.4)	111.6, CH		7.29, dd (7.6, 1.4)
9-OH									
10	131.4, C			142.7, C			136.4, C		
11-NH									
12	183.1, C			182.0, C			141.9, C		
13	43.2, C			41.9, C			40.1, C		
14	144.6, CH		6.08, dd (17.4, 10.5)	143.2, CH		6.06, dd (17.2, 10.9)	148.0, CH		6.17, dd (17.4, 10.5)
15	114.3, CH ₂		5.10, dd (10.5, 1.2)	112.9, CH ₂		5.07, dd (10.9, 1.2)	111.9, CH ₂		5.16, dd (17.4, 1.2)

			5.03, dd (17.4, 1.2)			4.97, dd (17.2, 1.2)			5.12, dd (10.5, 1.2)
16	22.3,	CH ₃	1.12, s	21.2,	CH ₃	1.10, s	28.6,	CH ₃	1.54, s
17	22.4,	CH ₃	1.04, s	20.9,	CH ₃	1.02, s	28.3,	CH ₃	1.54, s
1'	176.4,	C		174.9,	C		175.9,	C	
2'	74.5,	CH	3.98, dd (10.5, 2.3)	73.5,	CH	3.93, dd (10.3, 2.3)	74.0,	CH	4.01, dd (8.5, 3.4)
2'-OH									
3'	41.3,	CH ₂	2.90, dd (14.2, 2.3)	39.9,	CH ₂	2.87, dd (14.3, 2.3)	40.9,	CH ₂	2.51, dd (14.0, 3.4)
			2.68, dd (14.2, 10.5)			2.63, dd (14.3, 10.3)			2.06, dd (14.0, 8.5)
4'	140.4,	C		139.1,	C		139.2,	C	
5'/9'	130.5,	CH	7.29, d (7.3)	129.2,	CH	7.27, d (7.4)	130.4,	CH	6.93, m
6'/8'	129.1,	CH	7.24, dd (7.3)	127.8,	CH	7.23, t (7.4)	128.9,	CH	7.03, m
7'	127.2,	CH	7.16, dd (7.3)	125.8,	CH	7.16, t (7.4)	127.1,	CH	7.03, m

^a 400 MHz for ¹H and 100 MHz for ¹³C. ^b 500 MHz for ¹H and 125 MHz for ¹³C.

Compound **4** was isolated as a yellow oil. Its molecular formula was deduced as C₂₅H₂₈N₂O₅ based on the molecular ion peak at *m/z* 437.2087 [M + H]⁺ (IHD = 13) in the HRESIMS. Detailed analysis of the 1D and 2D NMR data (Figure 1 and Table 2) revealed that this compound was nearly identical to **3**: the key differences were the presence of an aromatic proton at C-9 [δ_{H} 6.83 (1H, d, *J* = 7.4 Hz) and δ_{C} 109.3] and a difference of 16 Da, suggesting that **1** lacks the phenolic hydroxy group at C-9. Thus, this compound was named 9-deoxy-*seco*-PF1233 B carboxylic acid (**4**).

Compound **5** was isolated as a pale yellow oil. The molecular formula was established as C₂₅H₂₈N₂O₄ according to its HRESIMS peak at *m/z* 421.2111 [M + H]⁺ (IHD = 13). The 1D and 2D NMR data (Table 2 and Figure 1) were similar to those of compounds **3**, **4**, and **8**, except for the following key changes: the methylene H₂-3 (δ_{H} 3.39, dd, *J* = 14.6, 5.3 Hz and 3.12, dd, *J* = 14.6, 10.4 Hz) was shifted to the low-field region in the ¹H NMR spectrum and showed strong HMBC correlations with the carbonyl carbon C-1 (δ_{C} 177.5) and the aromatic carbons C-12 (δ_{C} 141.9), C-4 (δ_{C} 106.8), and C-5 (δ_{C} 131.1) of the indole unit; the methine H-2 (δ_{H} 4.75,

dd, $J = 10.4, 5.3$ Hz) was also shielded and exhibited HMBC correlations with C-4, C-1, C-1' ($\delta_C 175.9$), and C-3 ($\delta_C 29.0$); the position of the isoprene unit at C-12 was confirmed by the HMBC correlations from H-14 ($\delta_H 6.17$, dd, $J = 17.4, 10.5$ Hz) to C-12, C-16 ($\delta_C 28.6$), and C-17 ($\delta_C 28.3$) and from H₃-16/17 ($\delta_H 1.54$, s) to C-12 and C-14 ($\delta_C 148.0$); finally, the oxygenated methine signal at $\delta_H 4.01$ (1H, d, $J = 8.5, 3.4$ Hz, H-2') revealed HMBC correlations to C-1' and C-4' ($\delta_C 139.2$) and from the methylene H₂-3' ($\delta_H 2.51$, dd, $J = 14.0, 3.4$ Hz and 2.06 , dd, $J = 14.0, 8.5$ Hz) with C-1' and C-5'/9' ($\delta_C 130.4$), consistent with a phenylpropanoic acid moiety. All the NMR data mentioned above suggested that compound **5** did not undergo the 1,2-sigmatropic rearrangement of the isoprene unit as in **3** and **4**(15) and as in the related dioxopiperazines deoxybrevianamide E and notoamide E.(24) Therefore, compound **5** was given the trivial name 4,9-dideoxy-*seco*-PF1233 B carboxylic acid (**5**).

Khalil and collaborators suggested *seco*-shornephine A methyl ester (**8**) was a methanolysis artifact of the solvolytically unstable PF1233 B (**6**) or shornephine A.(15) To determinate whether this is the case for derivatives **3–5**, we exposed **6** to MeOH and ACN + 0.1% formic acid conditions (see Experimental Section). The reaction products were analyzed by UPLC-ESIMS, and no hydrolysis or methanolysis products were detected either by comparison with pure samples of **3–5** or by selective molecular ion search at m/z 453 $[M + H]^+$ for **3**, 437 $[M + H]^+$ for **4**, 421 $[M + H]^+$ for **5**, and 467 $[M + H]^+$ and 489 $[M + Na]^+$ for **8** (Figures S37 and S38). In addition, the presence of **3–6** in the crude EtOAc extract (MeOH and acid free) of the fungal strain was demonstrated by UPLC-ESIMS analysis (Figure S39). In this experiment, **8** was also not found by selective molecular ion search. These findings prove that derivatives **3–5** are solvolytically stable and were produced as natural products by the fungus.

The relative configuration of **1** and **2** was established based on NOE correlations as indicated in Figure 1, and it was consistent with the absolute configuration reported for PF1233 B (**6**) or shornephine A by acid hydrolysis derivatization followed by ROESY analysis.(15) In this work, we used VCD, a nondegradative method, to establish the absolute configuration of **1** and **2** and used PF1233 B (**6**) to validate this method. This technique has recently become popular for the determination of absolute configuration of natural products.(25–28) The method is based on comparing IR and VCD experimental and calculated spectra. High enough similarity index values, S_{IR} and S_E , provide acceptable confidence levels for the absolute configuration assignment.(29)The molecular mechanics conformational search using the MMFF94 force field for compounds **1**, **2**, and **6** provided 94, 144, and 59 conformers, respectively, in a 10 kcal/mol range. Then, geometry optimization of the structures using density functional theory (DFT) with the B3PW91 functional and the DGDZVP basis set reduced the number of conformers to 35 for **1**, 55 for **2**, and 41 for **6**. Next, 19, 15, and 20 conformers within the first 3 kcal/mol, for **1**, **2**, and **6**, were selected for dipole moment and rotational strength calculation at the same level of theory. Free energy values allowed selecting nine conformers for **1**, seven for **2**, and eight for **6**, which resulted in conformational populations greater than 2% and represented 97.2%, 96.1%, and 93.4% of the total Boltzmann-weighted distribution, respectively (Table S1 and Figures S34–S36). Finally, calculated IR and VCD spectra (Figure 2) were obtained considering the weighting factors shown in Table S1. Comparison data in Table 3 show values greater than 96 for the S_{IR} indexes and show S_E values above 83, thus establishing the absolute configuration

with 100% confidence. Furthermore, low values of VCD spectra similarity for the incorrect enantiomer (S_{-E}) provided high enantiomeric selectivity indexes (ESI) for the absolute configuration determination of compounds **1**, **2**, and **6**. Since **3–5** have the same 2,3-substituted-indoline and 2-hydroxy-3-phenylpropanamide cores as **1**, **2**, and **6**, their absolute configuration was assumed based on biogenetic considerations.

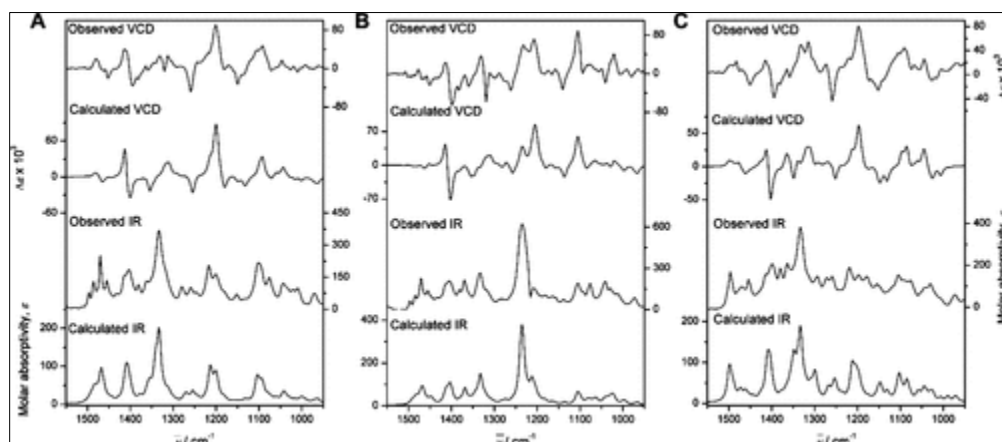


Figure 2. Comparison of the experimental and B3PW91/DGDZVP-calculated VCD and IR spectra of (2*S*,4*S*,12*R*,1'*S*)-**1** (A), (2*S*,4*S*,12*R*,1'*S*)-**2** (B), and (2*S*,4*S*,12*R*,1'*S*)-**6** (C).

Table 3. Confidence Level Data for the IR and VCD Spectra of **1, **2**, and **6****

compound	anH ^a	S_{IR}^b	S_E^c	S_{-E}^d	ESI ^e	C^f (%)
1	0.972	96.9	84.1	11.2	72.9	100
2	0.972	97.5	83.3	9.9	73.3	100
6	0.971	96.1	84.4	8.9	75.6	100

^a Anharmonicity factor. ^b IR spectral similarity. ^c VCD spectral similarity for the correct enantiomer. ^d VCD spectral similarity for the incorrect enantiomer. ^e Enantiomer similarity index, calculated as $S_E - S_{-E}$. ^f Confidence level for the stereochemical assignments.

The cytotoxic properties of derivatives **3**, **5**, and **6** were determined using a panel of human cancer cell lines with different functional status for p53 and against a cell line (A549/DXR) that overexpresses Pgp and presents developed resistance to doxorubicin (DXR). In the first case, all compounds were not cytotoxic ($IC_{50} > 50 \mu M$) after 72 h of treatment in the human cancer cell lines, regardless of the p53 functional condition (Figures S2 and S3). On the other hand, activity of the compounds against the A549/DXR cell line, measured by the fluorescent calcein-AM assay (Figure 3A) and cell viability (Figure 3C), showed a significant dose-dependent effect starting at 0.1 and 0.5 μM , respectively. In the control parental drug-sensitive A549 cells, which did not overexpress Pgp, compounds **3**, **5**, and **6** also reduced the efflux of calcein but starting at a 10 μM dose (Figure 3B). Similar effects were observed in mutant p53 breast cancer cell line MDA-MB-231 (Figures S4 and S5). Interestingly, the elimination of p53 mutant expression in an isogenic counterpart MDA-MB-231 p53CRISPR-Cas9 cell line abrogated the modest effect of **3**, **5**, and **6** on calcein accumulation. Furthermore, the combination of these compounds and

DXR also improved DXR-mediated cytotoxicity in other cancer cell lines in a p53-dependent manner (Figure S6).

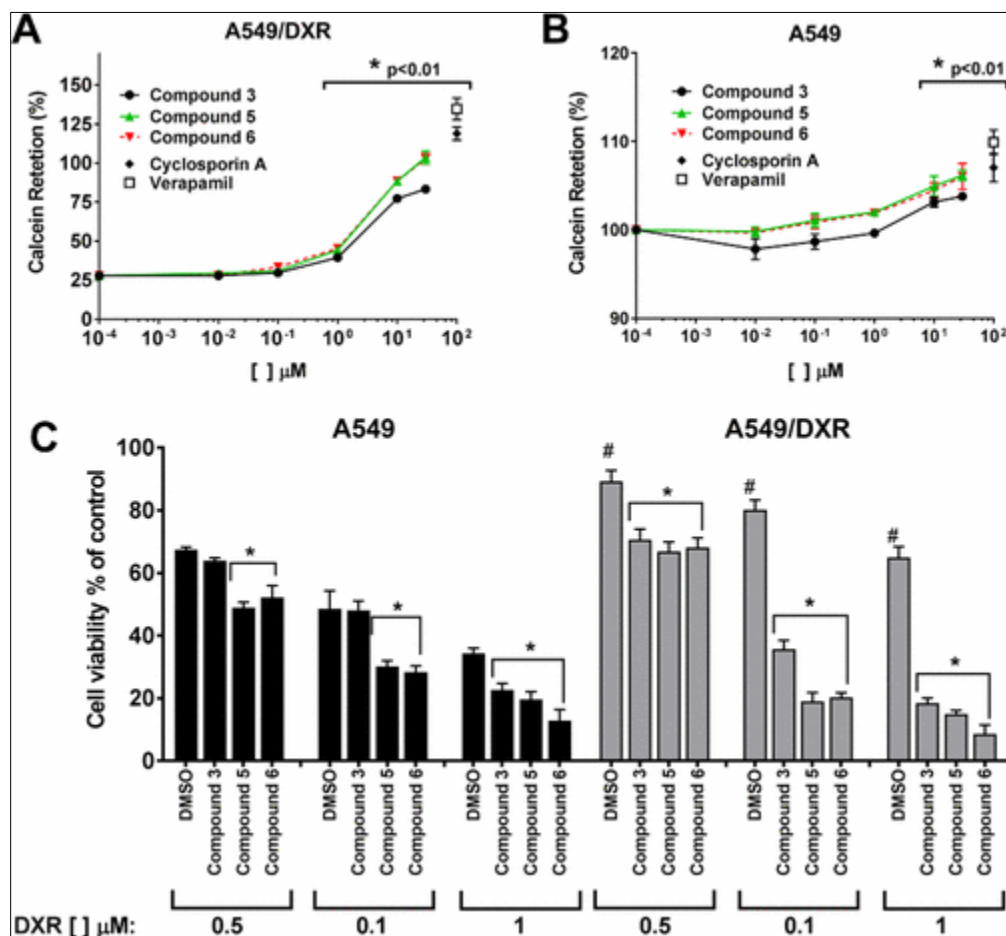


Figure 3. Effect of **3** (●), **5** (green ▲), and **6** (red ▼) on calcein-AM efflux from (A) A549/DXR and (B) A549 cells. Verapamil (□; 50 μg/mL) and cyclosporine A (◆; 25 μg/mL) were used as positive controls. (C) Activity of **3**, **5**, and **6** on DXR sensitivity in A549- and Pgp-overexpressing A549/DXR cells. Cells were treated with different concentrations of DXR alone or in combination with 10 μM of each compound for 72 h. Data represent the mean ± SEM of three independent experiments (**p*-value <0.01 relative to DMSO-treated samples; #*p*-value <0.01 when A549/DXR cells treated with DXR in the presence of vehicle DMSO are compared to its corresponding condition in A549 parental cells).

Experimental Section

General Experimental Procedures

UV spectra were acquired with a Shimadzu U160 spectrophotometer (Shimadzu Corp., Kyoto, Japan). IR spectra were obtained using a PerkinElmer Frontier IR 400 spectrometer (PerkinElmer, Waltham, MA, USA). The optical rotations were recorded at the sodium D-line wavelength on a PerkinElmer 343 polarimeter using a 1 cm cell at 22 °C. NMR data were collected using either a JEOL ECS-400 spectrometer (JEOL Ltd., Tokyo, Japan) equipped with a

high-sensitivity JEOL Royal probe and a 24-slot autosampler, a JEOL ECA-500 spectrometer, or an Agilent 700 MHz spectrometer (Agilent Tech., Santa Clara, CA, USA) equipped with a cryoprobe. LC-HRESIMS data were measured using a Thermo LTQ Orbitrap XL system (Thermo Fisher Scientific, Waltham, MA, USA) equipped with an electrospray ionization source, in both positive and negative ion modes, via an Acquity UPLC system (Waters, Milford, MA, USA). Low-resolution LC-ESIMS data were measured using a Waters SQD2 system (Waters) equipped with an electrospray ionization source, in both positive and negative ion modes, via an Acquity UPLC system (Waters). For both LC-MS analysis, a reversed-phase C₁₈ column (Waters BEH C₁₈ column, 50 × 2.1 mm i.d., 1.7 μm) was used with a gradient solvent system from 20:80 to 100:0 CH₃CN–H₂O (0.1% formic acid) in 10 min for HRESIMS or 12 min for LRESIMS, at a flow rate of 0.3 mL/min. Analytical and preparative HPLC were conducted on Gemini C₁₈ columns (5 μm, 110 Å, 250 × 4.6 mm i.d. and 5 μm, 110 Å, 250 × 21.2 mm i.d. for analytical and preparative runs, respectively; Phenomenex, Torrance, CA, USA) along with a Waters HPLC system comprising a 2535 quaternary pump, a 2707 autosampler, and using 2998 PDA and 2424 ELSD detectors. Data acquisition and management of chromatographic output were performed with the Empower 3 software (Waters). Silica gel 60 (70–230 mesh, Merck, Darmstadt, Germany) was used for column chromatography. Flash chromatography was accomplished on a CombiFlash Rf+ Lumen system (Teledyne Technologies, Inc., Lincoln, NE, USA) using RediSep Rf Gold Si-gel columns (Teledyne Technologies, Inc.). Reagent-grade chloroform, *n*-hexane, methanol, ethyl acetate, HPLC-grade acetonitrile, and water were purchased from J.T. Baker (Avantor Performance Materials, Center Valley, PA, USA). Deuterated NMR solvents were acquired from Cambridge Isotope Laboratories (Tewksbury, MA, USA).

Isolation and Identification of *Aspergillus* sp. MEXU 27854

Strain MEXU 27854 was isolated from sandy soil collected in the intertidal zone located in Caleta Bay, Acapulco, Guerrero, Mexico (16°49'53.92" N, 99°54'12.27" W) during January 2015. The strain was deposited at the fungal collection of Herbario Nacional de México, Universidad Nacional Autónoma de México (Mexico City), and identified as *Aspergillus* sp. based on the morphological characteristics and molecular sequence analysis ([Supporting Information](#)). The ITS (accession no. [KY406733](#)) and calmodulin (accession no. [KY407900](#) and [KY407901](#)) sequences were deposited in GenBank.

Fermentation, Extraction, and Isolation

The isolated *Aspergillus* sp. MEXU 27854 strain was cultivated on potato dextrose agar (PDA) plates. Agar plugs (1 cm) were inoculated in YESD (90 mL; 20 g of soy peptone, 20 g of dextrose, 5 g of yeast extract, 1 L of H₂O) media and incubated for 5 days at 22 °C, then separately transferred to a Fernbach flask with rice media (180 g/360 mL of H₂O). The fungus was grown on rice for 21 days and then extracted with 600 mL of 1:1 MeOH–CHCl₃. The mixture was shaken in a reciprocating shaker for 8 h and filtered, and then equal volumes of H₂O and CHCl₃ were added to the filtrate to a total volume of 1200 mL. Next, the mixture was stirred for 30 min and transferred into a separatory funnel. The bottom layer was drawn off and evaporated to dryness, and the obtained extract was defatted by stirring vigorously for 30 min in

a mixture of 180 mL of 1:1 MeOH–CH₃CN and 180 mL of *n*-hexane and then partitioned in a separatory funnel. The bottom layer was collected and evaporated to dryness to yield 885 mg of extract, which was subjected to fractionation by silica gel column chromatography using sequential mixtures of *n*-hexane–CHCl₃–MeOH to obtain five primary fractions. Fraction 2 (8.4 mg) was subjected to preparative HPLC using an isocratic elution solvent of 80% CH₃CN–H₂O (0.1% formic acid) at 21.24 mL/min, to yield **1** (0.8 mg, *t_R* = 4.1 min) and **2** (0.9 mg, *t_R* = 5.2 min). Fraction 3 (174 mg) was subjected to preparative HPLC using a gradient system from 40:60 to 100:0 of CH₃CN–H₂O (0.1% formic acid) in 15 min at 21.24 mL/min, yielding **6** (4 mg, *t_R* = 9.6 min). Fraction 4 (116 mg) was subjected to preparative HPLC using a gradient system from 35:65 to 100:0 of CH₃CN–H₂O (0.1% formic acid) in 15 min at 21.24 mL/min, yielding **3** (5.2 mg, *t_R* = 10.9 min), **4** (2.5 mg, *t_R* = 13.3 min), and **5** (2.1 mg, *t_R* = 14.5 min). In order to obtain more material, another fungal culture in 300 g of rice (600 mL of H₂O) was done under the same conditions, and 2.2 g of extract was obtained. This extract was fractionated via flash chromatography on a RediSep Rf Gold Si-gel column (24 g), using a gradient solvent system of *n*-hexane–CHCl₃–MeOH at 35 mL/min and 40 CV over 38.4 min. Fractions were collected every 23 mL and pooled into eight fractions according to their UV and ELSD profiles. Successive HPLC purifications from these fractions using the same procedures described above yielded additional amounts of **1** (21.1 mg), **2** (8.2 mg), **3** (3.0 mg), **4** (4.1 mg), **5** (5.2 mg), and **6** (37 mg). A third fermentation batch on rice (300 g of rice and 600 mL of H₂O) was prepared under the same conditions but extracted with 600 mL of ethyl acetate and defatted with *n*-hexane. The defatted extract was kept at 4 °C and subsequently analyzed by UPLC-ESI/MS for the presence of compounds **1–6** ([Supporting Information](#)).

9-Deoxy-PF1233 B (1):

yellow oil; [α]_D²⁵ +93 (*c* 0.1, MeOH); UV (MeOH) λ_{\max} (log ϵ) 207 (4.52), 276 (3.29), 294 (3.37) nm; FTIR ν_{\max} 3373, 3086, 3060, 3030, 2972, 2891, 1763, 1675, 1611, 1470, 1335 cm⁻¹; ¹H and ¹³C NMR, see [Table 1](#); HRESIMS *m/z* 419.1945 [M + H]⁺ (calcd for C₂₅H₂₇N₂O₄ 419.1965).

9-Deoxy-PF1233 A (2):

yellow oil; [α]_D²⁵ +160 (*c* 0.1, MeOH); UV (MeOH) λ_{\max} (log ϵ) 207 (4.47), 228 (3.89), 235 (3.91), 275 (3.36), 291 (3.39) nm; FTIR ν_{\max} 3366, 3027, 2975, 2928, 1765, 1680, 1608, 1470, 1410, 1336, 1230 cm⁻¹; ¹H and ¹³C NMR, see [Table 1](#); HRESIMS *m/z* 461.2052 [M + H]⁺ (calcd for C₂₇H₂₉N₂O₅ 461.2071).

seco-PF1233 B carboxylic acid (3):

yellow oil; [α]_D²⁵ –56 (*c* 0.1, MeOH); UV (MeOH) λ_{\max} (log ϵ) 208 (4.28), 273 (2.91), 298 (3.34) nm; FTIR ν_{\max} 3286, 3086, 3030, 2934, 1690, 1643, 1597, 1527, 1496, 1229 cm⁻¹; ¹H and ¹³C NMR, see [Table 2](#); HRESIMS *m/z* 453.2019 [M + H]⁺ (calcd for C₂₅H₂₉N₂O₆ 453.2020).

9-Deoxy-seco-PF1233 B carboxylic acid (4):

yellow oil; $[\alpha]_D^{25} -57$ (*c* 0.1, MeOH); UV (MeOH) λ_{\max} (log ϵ) 209 (4.33), 239 (3.69), 253 (3.72) nm; FTIR ν_{\max} 3288, 3079, 3035, 2912, 1720, 1651, 1603, 1519, 1240 cm^{-1} ; ^1H and ^{13}C NMR, see [Table 2](#); HRESIMS m/z 437.2081 $[\text{M} + \text{H}]^+$ (calcd for $\text{C}_{25}\text{H}_{29}\text{N}_2\text{O}_5$ 437.2071).

4,9-Dideoxy-*seco*-PF1233 B carboxylic acid (5):

yellow oil; $[\alpha]_D^{25} -23$ (*c* 0.1, MeOH); UV (MeOH) λ_{\max} (log ϵ) 207 (4.28), 213 (4.27), 225 (4.31), 254 (3.49), 282 (3.68) nm; FTIR ν_{\max} 3387, 3085, 3060, 3029, 2969, 2928, 1707, 1655, 1527, 1460, 1226, 1087, 920, 745, 701 cm^{-1} ; ^1H and ^{13}C NMR, see [Table 2](#); HRESIMS m/z 421.2111 $[\text{M} + \text{H}]^+$ (calcd for $\text{C}_{25}\text{H}_{29}\text{N}_2\text{O}_4$ 421.2122).

Stability of 6 in Methanol and Acid Conditions

Two different reaction vials containing 0.5 mg of **6** were set with either 500 μL of MeOH or acidified ACN (0.1% formic acid) and stirred at room temperature for 24 h. Aliquots from each reaction mixture were taken at 30 min and 8 h, and all the solutions were analyzed by UPLC-ESIMS for selective search of the molecular ions of **3–5** ([Supporting Information](#)).

Vibrational Circular Dichroism Measurements

IR and VCD spectra were measured in a dual PEM BioTools ChiralIR FT-VCD spectrophotometer operated at a resolution of 4 cm^{-1} . Samples of **1**, **2**, and **6** (10.1, 4.0, and 6.5 mg, respectively) were dissolved in 100% CDCl_3 (150 μL) and placed in a BaF_2 cell with a path-length of 100 μm . Six, 22, and 25 one hour blocks were added for measurements of **1**, **2**, and **6**, respectively. The baseline was generated by subtracting the spectrum of the solvent acquired under the same conditions. The samples' stability was monitored by ^1H NMR measurements immediately before and after VCD measurements.

Computational Methods

The molecular mechanics conformational search was done with the ComputeVOA software (BioTools, Jupiter, FL, USA). The conformers were submitted to Gaussian 09 (Gaussian, Inc., Wallingford, CT, USA) calculation for their geometry optimization performed using the B3PW91/DGDZVP level of theory. The PyMOL software (Schrödinger, LLC, New York, NY, USA) was used to discard identical geometries, using an alignment RMS smaller than or equal to 0.001 as the criterion. The conformers with relative energies within 3 kcal/mol, as compared to the most stable conformer, were considered to calculate vibrational frequencies, dipole transition moments, and rotational strengths. Individual IR and VCD spectra were obtained as the sum of Lorentzian bands with a half-width of 6 cm^{-1} for each frequency value. The final spectra were obtained considering the weighted IR and VCD spectra of conformers with a Boltzmann population greater than 2%, calculated using the free energy values. Comparison of calculated and experimental spectra was done with the CompareVOA software.

Cellular Viability Assay

HCT116 p53 $^{-/-}$ and p53 $^{+/+}$ cells were obtained from B. Vogelstein (John Hopkins University, Baltimore, MD, USA); MDA-MB-231 and MDA-MB-231 p53 CRISPR-Cas9 were kindly provided by Y. Ciribilli (University of Trento, Italy); U2OS (HTB96), SaOS2 (HTB85), A549

(CCL-185), and H1299 (CRL-5803D) were purchased from the American Tissue Culture Collection (ATCC). DXR-resistant A549 subline (A549/DXR) was developed by repeated exposure to stepwise increasing concentrations of DXR over a period of 4 months ([Supporting Information](#)). For the assays, cells were seeded into 96-well plates at 3000 to 4000 cells per well in 100 μL of growing medium and incubated for 20 h. Then the culture medium was replaced by 10% fetal bovine serum medium with the indicated concentrations of the selected compound or DXR for an additional 72 h. Cell viability was determined with the CellTiter 96 AQueous One Solution cell proliferation assay (Promega Corp., Madison, WI, USA) following the manufacturer's instructions. Optical densities were measured at 490 nm, using a Synergy2 multimode microplate reader (BioTek Instruments Inc., Winooski, VT, USA). Relative cell viability to untreated control cells was calculated. Triplicate wells were assayed for each condition.

Multidrug Resistance Assay

The Vybrant multidrug resistance assay kit (Thermo Fisher Scientific) was used to measure drug efflux inhibitory properties of the compounds in different cell lines following the manufacturer's recommendations. Briefly, drug-sensitive and drug-resistant cells (500 000 cells/well) were cultured in a 96-well plate overnight. Triplicate cell cultures were treated with the indicated concentrations of the selected compound and positive controls verapamil and cyclosporine A for 1 h and then incubated in 0.25 μM calcein-AM in 150 μL total volume. After 30 min, the cells were washed and centrifuged twice with 200 μL of cold culture medium. Intracellular calcein fluorescence was then measured with absorption maximum at 494 nm and emission maximum at 517 nm on a GloMax-Multi+ microplate multimode reader (Promega). Percentage of calcein retention was calculated following the manufacturer's guidelines.

Statistics

Data were graphed and statistically analyzed with the Graphpad Prism7 software (GraphPad Software Inc., La Jolla, CA, USA). Data represent the mean \pm SEM of at least three independent experiments. Statistically significant differences were identified using two-way ANOVA. *p*-Values of <0.01 were considered statistically significant.

Supporting Information

The Supporting Information is available free of charge on the [ACS Publications website](#) at DOI: [10.1021/acs.jnatprod.7b00331](https://doi.org/10.1021/acs.jnatprod.7b00331).

Additional experimental details, supporting references, morphology and phylogram analysis of *Aspergillus* sp. MEXU 27854, cytotoxic and calcein-AM assays of **3**, **5**, and **6** on different p53 functional status and MDR cancer cell lines, NMR, UPLC-PDA, and HRESIMS spectra of **1–6**, DFT B3PW91/DGDZVP minimum energy structures and relative energies and conformational populations of **1**, **2**, and **6**, and LCMS analysis of reaction products of **6** and EtOAc extract of the fungal strain ([PDF](#))

PDF [np7b00331_si_001.pdf \(4.92 MB\)](#)

‡Author Contributions

Taken in part from the Ph.D. thesis of Manuel A. Aparicio-Cuevas.

The authors declare no competing financial interest.

Acknowledgment

This work was supported by grants from CONACyT-CB 236564 and -INFRA 252226, and UNAM-DGAPA 205017 and -PAIP 5000-9145. We are indebted to Dirección General de Cómputo y de Tecnologías de Información y Comunicación (DGTIC), UNAM, for providing the resources to carry out computational calculations through the Miztli supercomputing system. M.A.A.-C. acknowledges a fellowship from CONACyT (274048) to pursue graduate studies. M.F. thanks R. Mata for her invaluable contributions to this work.

References

This article references 29 other publications.

1. Frisvad, J. C.; Larsen, T. O. *Front. Microbiol.* **2016**, 6, 1485 DOI: 10.3389/fmicb.2015.01485
2. Lee, Y. M.; Kim, M. J.; Li, H.; Zhang, P.; Bao, B.; Lee, K. J.; Jung, J. H. *Mar. Biotechnol.* **2013**, 15, 499– 519 DOI: 10.1007/s10126-013-9506-3
3. Konig, G. M.; Kehraus, S.; Seibert, S. F.; Abdel-Lateff, A.; Muller, D. *ChemBioChem* **2006**, 7, 229– 238 DOI: 10.1002/cbic.200500087
4. Zhao, C.; Liu, H.; Zhu, W. *Wei Sheng Wu Xue Bao* **2016**, 56, 331– 362
5. Overy, D. P.; Bayman, P.; Kerr, R. G.; Bills, G. F. *Mycology* **2014**, 5, 145– 167 DOI: 10.1080/21501203.2014.931308
6. Kushida, N.; Yaguchi, T.; Miike, N. Japan Patent JP2003096080, **2003**.
7. Dictionary of Natural Products, Online 25.2, <http://www.chemnetbase.com>; Taylor & Francis/CRC Press:London, UK, **2016**.
8. Iijima, M.; Masuda, T.; Nakamura, H.; Naganawa, H.; Kurasawa, S.; Okami, Y.; Ishizuka, M.; Takeuchi, T.; Iitake, Y. *J. Antibiot.* **1992**, 45, 1553– 1556 DOI: 10.7164/antibiotics.45.1553
9. Ola, A. R. B.; Aly, A. H.; Lin, W.; Wray, V.; Debbab, A. *Tetrahedron Lett.* **2014**, 55, 6184– 6187 DOI: 10.1016/j.tetlet.2014.09.048
10. Smelcerovic, A.; Yancheva, D.; Cherneva, E.; Petronijevic, Z.; Lamshoeft, M.; Herebian, D. *J. Mol. Struct.* **2011**, 985, 397– 402 DOI: 10.1016/j.molstruc.2010.11.029
11. Suntornchashwej, S.; Chaichit, N.; Isobe, M.; Suwanborirux, K. *J. Nat. Prod.* **2005**, 68, 951– 955 DOI: 10.1021/np0500124

12. Wang, H.; Gloer, J. B.; Wicklow, D. T.; Dowd, P. F. *J. Nat. Prod.* **1998**, 61, 804– 807 DOI: 10.1021/np9704056
13. Nakadate, S.; Nozawa, K.; Horie, H.; Fujii, Y.; Nagai, M.; Komai, S.-I.; Hosoe, T.; Kawai, K.-I.; Yaguchi, T.; Fukushima, K. *Heterocycles* **2006**, 68, 1969– 1972 DOI: 10.3987/COM-06-10804
14. Abe, M.; Yamano, T.; Yamatodani, S.; Kōzu, Y.; Kusumoto, M.; Komatsu, H.; Yamada, S. *Bull. Agric. Chem. Soc. Jpn.* **1959**, 23, 246– 248 DOI: 10.1271/bbb1924.23.246
15. Khalil, Z. G.; Huang, X. C.; Raju, R.; Piggott, A. M.; Capon, R. J. *J. Org. Chem.* **2014**, 79, 8700– 8705 DOI: 10.1021/jo501501z
16. Gottesman, M. M.; Fojo, T.; Bates, S. E. *Nat. Rev. Cancer* **2002**, 2, 48– 58 DOI: 10.1038/nrc706
17. Szakacs, G.; Paterson, J. K.; Ludwig, J. A.; Booth-Genthe, C.; Gottesman, M. M. *Nat. Rev. Drug Discovery* **2006**, 5, 219– 234 DOI: 10.1038/nrd1984
18. Muller, P. A.; Vousden, K. H. *Nat. Cell Biol.* **2013**, 15, 2– 8 DOI: 10.1038/ncb2641
19. Pflaum, J.; Schlosser, S.; Muller, M. *Front. Oncol.* **2014**, 4, 285 DOI: 10.3389/fonc.2014.00285
20. Chin, K. V.; Ueda, K.; Pastan, I.; Gottesman, M. M. *Science* **1992**, 255, 459– 462 DOI: 10.1126/science.1346476
21. Bradshaw, T. D.; Chua, M. S.; Orr, S.; Matthews, C. S.; Stevens, M. F. *Br. J. Cancer* **2000**, 83, 270– 277 DOI: 10.1054/bjoc.2000.1231
22. Sampath, J.; Sun, D.; Kidd, V. J.; Grenet, J.; Gandhi, A.; Shapiro, L. H.; Wang, Q.; Zambetti, G. P.; Schuetz, J. D. *J. Biol. Chem.* **2001**, 276, 39359– 39367 DOI: 10.1074/jbc.M103429200
23. Kanagasabai, R.; Krishnamurthy, K.; Druhan, L. J.; Ilangovan, G. *J. Biol. Chem.* **2011**, 286, 33289– 33300 DOI: 10.1074/jbc.M111.249102
24. Kato, H.; Nakamura, Y.; Finefield, J. M.; Umaoka, H.; Nakahara, T.; Williams, R. M.; Tsukamoto, S. *Tetrahedron Lett.* **2011**, 52, 6923– 6926 DOI: 10.1016/j.tetlet.2011.10.065
25. Batista, J. M., Jr; da Silva, B. V. In *Studies in Natural Products Chemistry*; Atta-ur-Rahman, Ed.; Elsevier:Amsterdam, **2015**; Vol. 41, pp 311– 451.
26. Batista, J. M., Jr.; Blanch, E. W.; da Silva, B. V. *Nat. Prod. Rep.* **2015**, 32, 1280– 1302 DOI: 10.1039/C5NP00027K
27. Burgueno-Tapia, E.; Joseph-Nathan, P. *Nat. Prod. Commun.* **2015**, 10, 1785– 1795

28. Joseph-Nathan, P.; Gordillo-Román, B. In *Progress in the Chemistry of Organic Natural Products*; Kinghorn, A. D.; Falk, H.; Gibbons, S.; Kobayashi, J., Eds.; Springer International Publishing: Basel, Switzerland, **2015**; Vol. 100, pp 311– 451.
29. Burgueno-Tapia, E.; Zepeda, L. G.; Joseph-Nathan, P. *Phytochemistry* **2010**, 71, 1158– 1161 DOI: 10.1016/j.phytochem.2010.04.005